

$^2J, ^3J$ -HMBC: A New Long-Range Heteronuclear Shift Correlation Technique Capable of Differentiating $^2J_{\text{CH}}$ from $^3J_{\text{CH}}$ Correlations to Protonated Carbons

V. V. Krishnamurthy,*¹ David J. Russell,[†] Chad E. Hadden,[†] and Gary E. Martin^{†1}

*Varian, Inc., NMR Applications Laboratory, Palo Alto, California 94303; and [†]Pharmaceutical Development, Rapid Structure Characterization Group, Pharmacia & Upjohn, Kalamazoo, Michigan 49001-0199

Received March 20, 2000; revised June 8, 2000

The development of a series of new, accordion-optimized long-range heteronuclear shift correlation techniques has been reported. A further derivative of the constant time variable delay introduced in the IMPEACH-MBC experiment, a STAR (Selectively Tailored Accordion F_1 Refocusing) operator is described in the present report. Incorporation of the STAR operator with the capability of user-selected homonuclear modulation scaling as in the CIGAR-HMBC experiment, into a long-range heteronuclear shift correlation pulse sequence, $^2J, ^3J$ -HMBC, affords for the first time in a proton-detected experiment the means of unequivocally differentiating two-bond ($^2J_{\text{CH}}$) from three-bond ($^3J_{\text{CH}}$) long-range correlations to protonated carbons. © 2000 Academic Press

Key Words: accordion excitation; long-range heteronuclear shift correlation; $^2J, ^3J$ -HMBC; constant time variable delay; STAR operator.

INTRODUCTION

Nuclear magnetic resonance (NMR) has assumed a role of paramount importance in the elucidation of unknown chemical structures, e.g., natural products, since the development of 2D NMR in the late 1970s. Further, long-range heteronuclear shift correlation methods have become increasingly important for the unequivocal linkage of contiguous protonated carbon segments to quaternary carbon and nitrogen atoms. Likewise, long-range heteronuclear shift correlation methods also provide the capability of orienting structural segments across NMR-silent heteroatoms such as oxygen and sulfur. Studies performed in the early 1980s relied on a rather diverse assortment of heteronucleus-detected methods, which have been reviewed (1). Heteronucleus-detected experiments have been almost completely supplanted by the proton- or inverse-detected HMBC experiment of Bax and Summers (2) reported in 1986 or still more recently by the gradient-HMBC (GHMBC) version of the experiment described by John and Hurd (3) in 1991.

Until recently, long-range heteronuclear shift correlation

experiments have been individually optimized for an arbitrarily selected value for the long-range delay in the experiment. Typically utilized optimizations have generally been in the range of from 6 to 10 Hz. Pioneering work by Wagner and Berger (4) in 1998 introduced the concept of “accordion”-optimization of the delays used to sample long-range heteronuclear couplings. The ACCORD-HMBC experiment devised by Wagner and Berger effectively allowed an investigator to “integrate” across a range of potential long-range heteronuclear couplings in a single experiment. Counterbalancing the ability to sample a broad range of potential long-range couplings is the F_1 “skew” of responses in ACCORD-HMBC experiments. F_1 response “skew” arises as a result of the variable delay in accordion-optimized experiments serving as a pseudo third evolution time for homonuclear coupling modulations. Martin, *et al.* (5) in a detailed study of the ACCORD-HMBC experiment have shown that the extent of F_1 skew is a function of the optimization range being sampled, the spectral width in F_1 , and the number of increments performed to digitize the second frequency domain.

Expanding on the idea of accordion-optimization of long-range delays, Hadden *et al.* (6) developed a new pulse sequence element known as a constant time variable delay. Functionally, this pulse sequence element [1] suppresses F_1 skew since

$$D/2 - 180^\circ 13\text{C} - D/2 - \text{vd} \quad [1]$$

homonuclear couplings evolve in constant time during the “constant time variable delay” for all increments of the evolution time (t_1); i.e., the constant time variable delay is incapable of serving as a pseudo third evolution time for homonuclear coupling modulations. In contrast, heteronuclear couplings, which are refocused during D, experience a variable delay, vd, in a fashion analogous to the ACCORD-HMBC experiment. The constant time variable delay has been incorporated into a pulse sequence given the acronym IMPEACH-MBC (6). Comparison of the results obtained with identically optimized,

¹ To whom correspondence may be addressed.

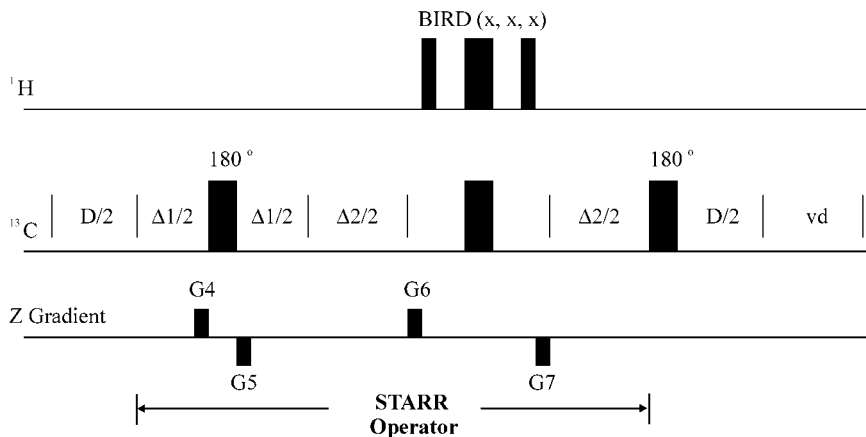


FIG. 1. STAR (Selectively Tailored Accordion F_1 Refocusing) operator from the $^2J, ^3J$ -HMBC experiment. This pulse sequence operator is introduced midway (either prior to the ^{13}C 180° pulse—as shown—or after the ^{13}C 180° pulse) through the D delay in the constant time variable delay element. The STAR operator consists of two variable delays ($\Delta 1$ and $\Delta 2$) the sum of which is held constant throughout the experiment. The $\Delta 1$ delay increases from zero to $J_{\text{scale}} * t_{1\text{max}}$ in steps of $J_{\text{scale}} * t_1$ synchronous with the t_1 evolution period. Whereas the $\Delta 2$ delay decreases from $J_{\text{scale}} * t_{1\text{max}}$ to zero in steps of $J_{\text{scale}} * t_1$ synchronous with t_1 evolution time. The ^{13}C 180° pulse midway through the $\Delta 1$ delay refocuses the heteronuclear long-range coupling while allowing ALL the homonuclear couplings to the “active” proton to evolve. The BIRD pulse midway through the $\Delta 2$ delay acts as a selective 180° pulse for ^{13}CH and as a 360° pulse for ^{12}CH protons. As a result, the homonuclear vicinal coupling $^3J^{12}\text{C}_2\text{H}-^{13}\text{C}_1\text{H}$ (see **1**) is decoupled by the action of the BIRD pulse while other homonuclear vicinal couplings; e.g., $^3J^{12}\text{C}_3\text{H}-^{12}\text{C}_2\text{H}$ are unaffected and continue to evolve through the $\Delta 2$ interval. The net effect of the operation of the BIRD pulse is thus to let the vicinal homonuclear coupling for a two-bond CH cross peak to evolve ONLY during a variable delay $\Delta 1$ thereby causing the long-range two-bond correlation responses to protonated carbons to be skewed in F_1 as illustrated schematically in Fig. 2 and Table 1 and experimentally verified by the data shown in the expanded panel of Fig. 4. Although the value of J_{scale} can be set to 0 or 1, as in the CIGAR-HMBC experiment (7), in most circumstances it will be desirable to set this parameter to >1 . Typically, in our experience we have found setting $J_{\text{scale}} \sim 15$ to provide usable results. The gradients flanking the ^{13}C 180° pulse and the BIRD pulses are to suppress any possible multiple quantum magnetization created by imperfections and/or offset effect of the ^{13}C 180° pulse. They are arbitrarily set pairwise (around 10 G/cm) provided that the pair sums to zero.

digitized, and processed ACCORD-HMBC and IMPEACH-MBC experiments showed the latter to be capable of suppressing F_1 skew, with the exception of the slight homonuclear coupling modulation during the evolution time, t_1 . The modulation during t_1 incrementation is analogous to that observed in conventional HMBC experiments. While the IMPEACH-MBC experiment potentially enhances the utility of accordion-optimized long-range experiments by eliminating the possibility of response overlap in F_1 due to skew, the IMPEACH-MBC experiment also unfortunately precludes the use of response skew in F_1 as a determinant of response authenticity (5).

Further modification of the constant time variable delay was incorporated into the subsequent generation of accordion-optimized experiments in a pulse sequence given the acronym CIGAR-HMBC (7). To restore the ability of F_1 skew to be employed for response authentication, the constant time variable delay was modified as shown by

$$(D/2 + \Delta 2/2) - 180^\circ {}^{13}\text{C} - (D/2 + \Delta 2/2) - \text{vd}. \quad [2]$$

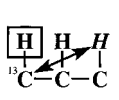
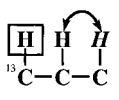
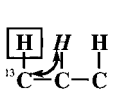
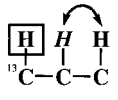
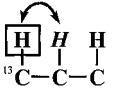
The variable delay, vd, is decremented in the accordion fashion from τ_{max} to τ_{min} ($1/2J_{\text{min}}$ and $1/2J_{\text{max}}$, respectively) in steps of $(\tau_{\text{max}} - \tau_{\text{min}})/ni$ (where ni corresponds to the number of increments of the evolution time used to digitize the second time domain). The delay D is incremented (from zero) according to

$$(\tau_{\text{max}} - \tau_{\text{min}})ni + \Delta 2, \quad [3]$$

where $\Delta 2$ is defined as $(J_{\text{scale}} - 1) * t_1$, where J_{scale} is the user-selected scaling parameter and t_1 is the evolution time. When $J_{\text{scale}} = 1$, (hence $\Delta 2 = 0$) the homonuclear modulation in the CIGAR-HMBC experiment is identical to that in an IMPEACH-MBC or HMBC experiment. When $J_{\text{scale}} = 0$, all homonuclear coupling modulation in F_1 is suppressed in a manner analogous to that of the CT-HMBC experiments recently proposed by Furihata and Seto (8). However, when $J_{\text{scale}} > 1$, a user-determined degree of F_1 skew is introduced into multiplet structure in the second frequency domain (see Panel D, Fig. 6), allowing the skew to be used as a determinant of response authenticity without concern for response overlap in F_1 , which can be troublesome in ACCORD-HMBC experiments.

The present report describes a further modification of the idea of the constant time variable delay introduced in the IMPEACH-MBC experiment (6) and modified in the CIGAR-HMBC experiment (7) described above. The key feature of CIGAR-HMBC is the user-definable (including zero) J -scaling of the cross peak along the F_1 domain by the homonuclear coupling. In this report, user-definable (typically >1) J -scaling of the cross peak along the F_1 dimension is used to differentiate two-bond ($^2J_{\text{CH}}$) and three-bond ($^3J_{\text{CH}}$) HMBC cross peaks to a protonated carbon. This pulse sequence element has

TABLE 1
Evolution of Various Components of Homo- and Heteronuclear Magnetization during the Various Delays
of the STAR Operator Used in ${}^2J_{\text{CH}}, {}^3J_{\text{CH}} = \text{HMBC}$

STAR operator delay interval	Three-bond couplings (${}^3J_{\text{CH}}$)		Two-bond couplings (${}^2J_{\text{CH}}$)		
					
D	Refocused	Evolve	Refocused	Evolve	Evolve
$\Delta 1$	Refocused	Evolve	Refocused	Evolve	Evolve
$\Delta 2$	Refocused	Refocus	Refocused	Evolve	Refocused
vd	Evolve	Evolve	Evolve	Evolve	Evolve

Note. \square Experiences a π pulse midway through $\Delta 1$; ${}^{13}\text{C}$ Experiences a π pulse midway through $\Delta 1$, $\Delta 2$, and D.

been given the acronym STAR (Selectively Tailored Accordion F_1 Refocusing) operator and serves to allow the unequivocal differentiation of two-bond from three-bond long-range heteronuclear couplings to protonated carbons. This is the first example of a proton-detected long-range correlation experiment to offer this capability, which had been previously described by Reynolds *et al.*, (9) in their report of the XCORFE, heteronucleus-detected long-range correlation experiment.

THE STAR OPERATOR

The STAR (Selectively Tailored Accordion F_1 Refocusing) operator is shown in Fig. 1. This new pulse sequence operator has some component segments in common with the constant time variable delay introduced in the IMPEACH-MBC experiment (6, 7). The STAR operator is also a “constant time variable delay.” The delay $\Delta 1$ is incremented from zero to $J_{\text{scale}} * t_{1\text{max}}$ in steps of $J_{\text{scale}} * t_1$ while the $\Delta 2$ delay is decremented from $J_{\text{scale}} * t_{1\text{max}}$ to zero in steps of $J_{\text{scale}} * t_1$ (where t_1 is the F_1 incremental delay and $t_{1\text{max}}$ is the “acquisition time” in the evolution dimension) synchronous with the t_1 incrementation. While the sum of $\Delta 1$ and $\Delta 2$ is a constant, the individual delays $\Delta 1$ and $\Delta 2$ are variable and are a function of the evolution delay, t_1 . This results in three possible scenarios: (i) any coupling that evolves during one of the two delays ($\Delta 1$ or $\Delta 2$), but is refocused during the other will modulate the F_1 response by a factor $J_{\text{scale}} * J$; (ii) any coupling that evolves during both $\Delta 1$ and $\Delta 2$ will not have any effect on the F_1 response; and (iii) any coupling that is refocused during both $\Delta 1$ and $\Delta 2$ will not have any effect on the F_1 response. The ${}^{13}\text{C}$ 180° pulse midway through the $\Delta 1$ delay in the STAR operator refocuses the heteronuclear long-range coupling during this interval but lets ALL homonuclear couplings continue to evolve. The BIRD pulse midway through the $\Delta 2$ delay behaves as a 180° pulse for the ${}^{13}\text{C}$ and the proton(s) that is directly attached to it, but as a 0° pulse for all other protons, including the “active” proton of a long-range CH spin pair. The function of the BIRD pulse is similar to that of the BIRD pulse centered

in the $\Delta 2$ refocusing delay of the XCORFE pulse developed by Reynolds and co-workers in 1985 (9). To delineate the behavior of the F_1 response of a given long-range CH spin pair, one needs to investigate the fate of the homo and heteronuclear couplings to the “active” H1 spin during the $\Delta 1$ and $\Delta 2$ intervals.

Table 1 summarizes the behavior of homo- and heteronuclear couplings for a two-bond and three-bond (or n -bond, where $n > 2$) correlation. For completeness their behavior during the D and the vd delays (the delays in the “Constant Time Variable Delay”) are also included. For both ${}^2J_{\text{CH}}$ and ${}^3J_{\text{CH}}$ correlations the ${}^1\text{H}$ - ${}^{13}\text{C}$ heteronuclear coupling is refocused during $\Delta 1$, $\Delta 2$, and D, but evolves only during the variable delay vd thus retaining the accordion sampling of a

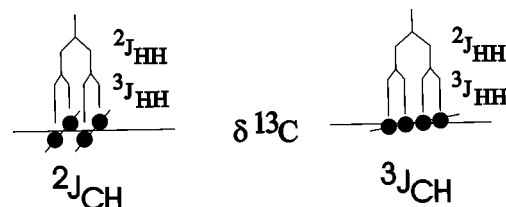


FIG. 2. Schematic showing the effect of the BIRD pulse located midway through the $\Delta 2$ interval of the STAR operator (Fig. 1). The vicinal component of magnetization in the long-range response that is two-bond coupled to a protonated carbon (${}^3J_{\text{HH}}$ (coupling A, see 1) experiences modulation during $\Delta 1$, which serves as pseudo evolution for this coupling, due to the selective refocusing effect of the BIRD pulse during $\Delta 2$. Evolution of ${}^3J_{\text{HH}}$ (coupling A, see 1) during a variable $\Delta 1$ interval causes this component of a long-range correlation response to be “skewed” in F_1 in a manner analogous to responses in the ACCORD-HMBC experiment (5). In contrast, the three-bond homonuclear vicinal coupling, ${}^3J_{\text{HH}}$ (coupling B, see 1), is unaffected by the BIRD pulse. Thus, the proton of this homonuclear pair coupled via a three-bond heteronuclear coupling to a protonated carbon is unaffected by the action of the BIRD pulse and evolves during a constant delay ($\Delta 1 + \Delta 2$). Consequently, the three-bond long-range heteronuclear correlation does not exhibit an F_1 skew to any of its components of magnetization, leaving the response “normal.” Homonuclear modulation during the evolution period, t_1 , is still present as in HMBC/GHMBC (2, 3) and IMPEACH-MBC (6) experiments, which is depicted as the slight F_1 “skew” of the ${}^3J_{\text{CH}}$ correlation response.

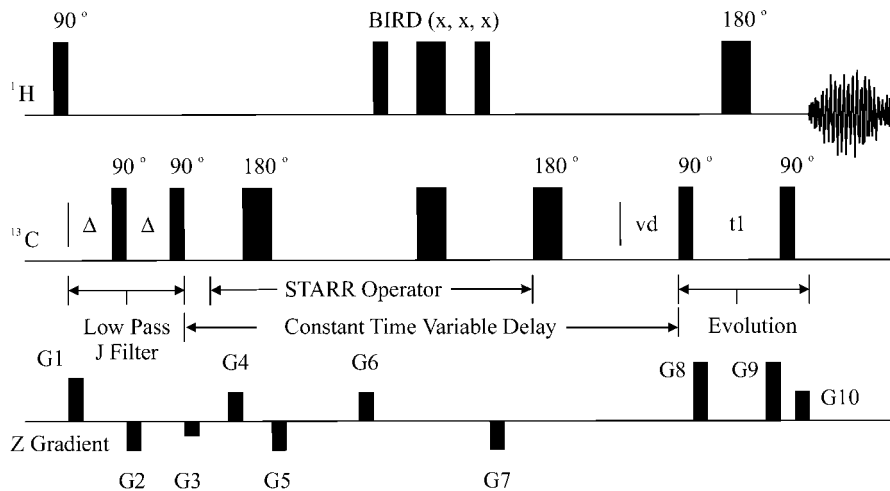
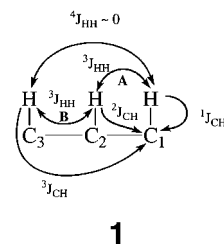


FIG. 3. Pulse sequence for the ${}^2J, {}^3J$ -HMBC experiment. The experiment begins with a dual-stage gradient low-pass J -filter (7). The associated z -gradient pulses, G1, G2, and G3, can be arbitrarily set as a trio, e.g. 15, -10 , -5 , provided the three gradients sum to zero. The complete details of the STAR operator incorporated in the pulse sequence are presented in Fig. 1. The setting of z -gradient pulses within the STAR operator (G4–G7) is discussed in Fig. 1. The variable delay, vd , is decremented in accordion fashion from an initial value of $\tau_{\max} (1/2^n J_{\min})$ to $\tau_{\min} (1/2^n J_{\max})$ in steps of $(\tau_{\max} - \tau_{\min})/ni$, where ni corresponds to the number of t_1 increments being performed to digitize the second time domain. The delay interval D , is correspondingly incremented by the same amount. Following the constant time variable delay, the experiment operates in the usual fashion of a GHMBC experiment (2, 3) with the coherence pathway selected by z gradients G8–G10, which are applied in the ratio 2:2:1 or a corresponding equivalent for ${}^1\text{H}$ – ${}^{13}\text{C}$ experiments. Gradients employed were as follows: dual stage low-pass J -filter (G1–G3) 10, -6.63 , -3.37 G cm^{-1} , respectively; STAR operator (G4–G7) 20, -20 , 20, -20 G cm^{-1} , respectively; coherence selection gradients (G8–G10) 5, 5, 2.52 G cm^{-1} , respectively. A simple four step phase cycle was employed; phases are zero unless otherwise noted: $\phi_1 = \phi_r = 0202$.

range of couplings. For a two-bond cross peak to a protonated carbon the vicinal ${}^1\text{H}$ – ${}^1\text{H}$ coupling between the “active” proton and the proton attached to the ${}^{13}\text{C}$ evolves during $\Delta 1$, D , and vd but is refocused during the variable delay $\Delta 2$. This introduces a J_{scale} -dependent F_1 skew in the two-bond cross peaks. For a three-bond cross peak, the homonuclear coupling between the “active” proton and the proton attached to the “active” carbon is typically zero. The ${}^1\text{H}$ – ${}^1\text{H}$ coupling between the “active” proton and all other protons evolves during all four delays. Since $\Delta 1 + \Delta 2$ (as well as $D+vd$) is a constant for all increments, this evolution during a constant delay does not cause any modulation of the F_1 response.

Differential behavior of the two-bond and three-bond correlations is best illustrated using the hypothetical fragment as shown by **1**. The BIRD pulse midway through $\Delta 2$ serves as a 180° pulse for H_1 and C_1 , but as a 360° pulse for H_2 and H_3 . Both long-range heteronuclear couplings, ${}^2J_{\text{CH}}$ and ${}^3J_{\text{CH}}$, are refocused during $\Delta 2$. They are also refocused during $\Delta 1$ due to the ${}^{13}\text{C}$ 180° pulse midway through $\Delta 1$. The homonuclear coupling between H_3 and H_2 evolves during $\Delta 1$ and $\Delta 2$ (i.e., during a constant delay $\Delta 1 + \Delta 2$) and hence modulates neither the two-bond nor the three-bond cross peak between H_2 – C_1 and H_3 – C_1 , respectively. The behavior of these couplings will be very similar to what is observed in IMPEACH-MBC (6) or CIGAR-HMBC (7) with $J_{\text{scale}} = 1$. The homonuclear coupling between H_2 and H_1 is refocused during $\Delta 2$ due to the differential effect of the BIRD pulse on ${}^{13}\text{C}_1$ and ${}^{12}\text{C}_2$ attached protons. However, H_2 – H_1 coupling continues to evolve during $\Delta 1$, a variable delay that serves as a pseudo evolution. Hence

the behavior of this coupling will be very similar to what will be observed in CIGAR-HMBC with $J_{\text{scale}} > 1$ and will selectively introduce a F_1 skew in ${}^2J_{\text{CH}}$ correlation responses to protonated carbons.



1

The expected response behavior resulting from the action of the STAR operator on a two-bond vs. a three-bond long-range correlation response is illustrated schematically in Fig. 2. As is shown in the multiplet represented on the left in Fig. 2, the homonuclear vicinal coupling component of magnetization is skewed in F_1 about the chemical shift of the carbon to which the proton has a two-bond (${}^2J_{\text{CH}}$) heteronuclear coupling. The three-bond (${}^3J_{\text{CH}}$) heteronuclear correlation response depicted to the right in the Fig. 2, in contrast, does not exhibit any skew in F_1 for the vicinal coupling component of that multiplet since this specific homonuclear vicinal coupling was allowed to evolve normally by the BIRD pulse. The experimental verification of this schematic representation is presented below in Fig. 4.

During the development and experimental testing of the

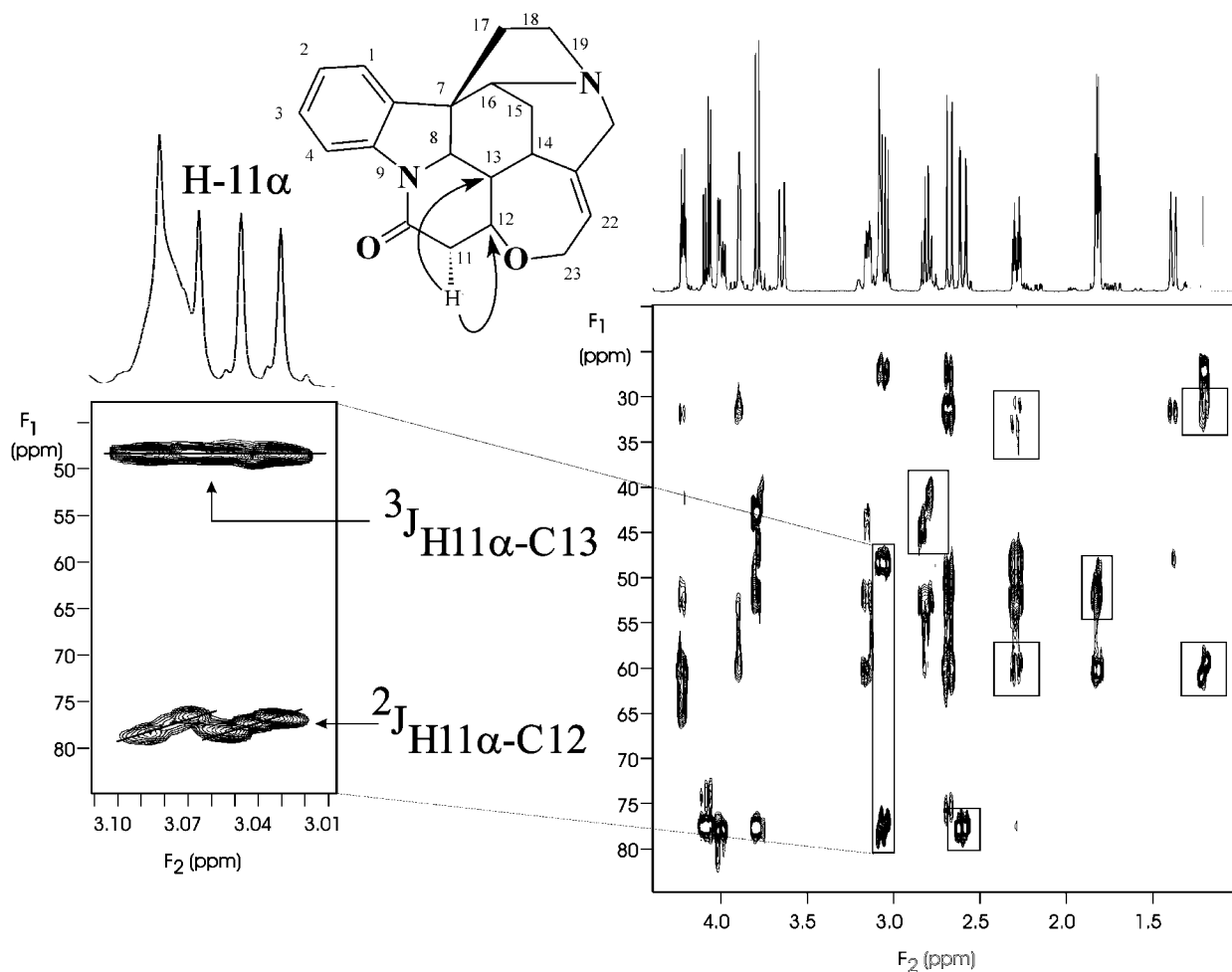


FIG. 4. ${}^2J, {}^3J$ -HMBC spectrum of strychnine (**2**). The experiment was accordion-optimized for long-range couplings in the range of 6–10 Hz. The J_{scale} parameter was set to 16. Data were acquired as 2048×128 files with spectral widths in F_2 and F_1 of 4454 and 28,269 Hz, respectively. The accordion optimization range was from 6 Hz (83.3 ms) to 10 Hz (50.0 ms). The strychnine (**2**) data shown were acquired using $J_{\text{scale}} = 16$. The initial value of the delays in the STAR operator were: $\text{vd} = 83.3$ ms; $D = 0$; $\Delta 1 = 0$; $\Delta 2 = J_{\text{scale}} * t_{1\text{max}}$. The delays within the STAR operator were manipulated over the course of the experiment such that: $\Delta 1$ was incremented to $J_{\text{scale}} * t_{1\text{max}}$; $\Delta 2$ was decremented to zero. These manipulations keep the overall duration of the STAR operator constant over the course of the experiment. The delays D and vd were manipulated such that $D = 33.3$ ms for the final increment of the evolution time and $\text{vd} = 50$ ms for the final increment. Data were linear predicted to a total of 256 points in the second time domain before zero-filling and Fourier transformation to afford a final data matrix consisting of 2048×512 points. Squared sinebell multiplication, the time constants adjusted to the acquisition time in both domains, was used prior to both Fourier transformations. The long-range correlations from the H-11 α resonance to C-12 (${}^2J_{\text{CH}}$) and C-13 (${}^3J_{\text{CH}}$) are shown in the expanded spectral segment in the separate panel. These responses illustrate the experimental verification of the expected multiplet structure as shown schematically in Fig. 2. Other two-bond long-range correlations are shown in the boxed regions of the aliphatic portion of the spectrum.

STAR operator, it was found that in some cases the F_1 skew (without any J scaling) exhibited by ${}^2J_{\text{CH}}$ long-range correlation responses was rather subtle and difficult to discern. For this reason, the STAR operator was further modified in a fashion analogous to the CIGAR-HMBC experiment (7) through the incorporation of a J_{scale} parameter to augment the degree of “skew” for two-bond long-range couplings, as noted above. Its purpose is to intentionally introduce additional homonuclear modulation during $\Delta 2$ by allowing for longer “pseudo evolution” of the desired component of magnetization, i.e., ${}^2J_{\text{CH}}$. The increase in the duration of the pseudo evolution time available correspondingly increases the F_1 “skew” of the

heteronuclear ${}^2J_{\text{CH}}$ components of magnetization making them easier to discern visually. The use of J scaling to increase the apparent J modulation along an evolution dimension is similar to the use of scaling factors by Krishnamurthy (10, 11), Furihata and Seto (12), Permi *et al.* (13), and Williamson and co-workers (14).

RESULTS AND DISCUSSION

The complete ${}^2J, {}^3J$ -HMBC pulse sequence is shown in Fig. 3. Applying this experiment to strychnine (**2**) gave the experimental result shown in Fig. 4. The data were acquired using a

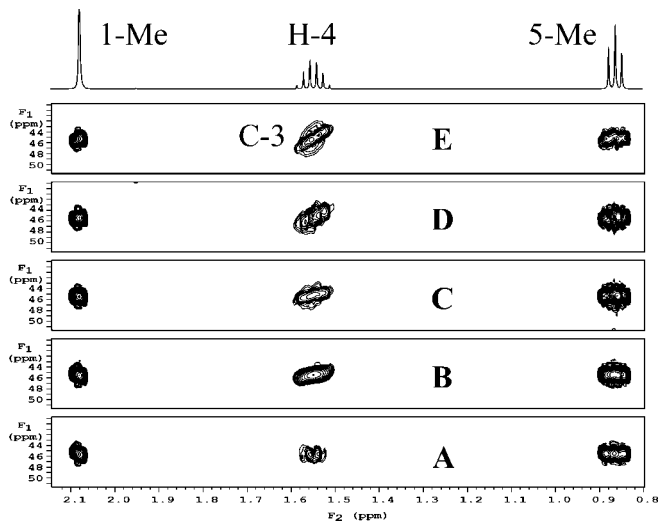
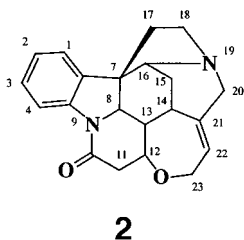


FIG. 5. Segments of ${}^2J, {}^3J$ -HMBC spectra of 2-pentanone (**3**) accordion-optimized for long-range couplings in the range of 6–10 Hz. The data were acquired as 2048×128 point files, accumulating 20 transients/ t_1 increment. Data were linear predicted to 256 points in t_1 prior to Fourier transformation; squared sinebell multiplication was employed in both time domains. The experiments were identically parameterized with the exception of the parameter J_{scale} which was varied from $J_{\text{scale}} = 0$ (panel A), to $J_{\text{scale}} = 6$ (panel B), to $J_{\text{scale}} = 12$ (panel C), $J_{\text{scale}} = 18$ (panel D), and finally to $J_{\text{scale}} = 24$ (panel E). As will be noted, the three-bond correlations from the 1-methyl and 5-methyl resonances to C-3 are unaffected by the alteration of J_{scale} . In contrast, the F_1 skew introduced by the STAR operator into the ${}^2J_{\text{CH}}$ coupling from the 4-methylene resonance to C-3 becomes more pronounced as the value used for J_{scale} is increased.

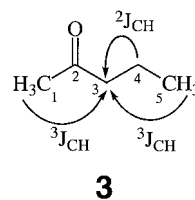
6–10 Hz accordion optimization and $J_{\text{scale}} = 16$. Experimental verification of the anticipated multiplet structure shown in Fig. 2 is readily provided by the responses for the correlations of H11 α to C12 (${}^2J_{\text{CH}}$) and C13 (${}^3J_{\text{CH}}$) shown in the expanded panel extracted from the spectrum. Other two-bond long-range correlations observed in the aliphatic region of the spectrum are designated with boxes. Not all of the possible ${}^2J_{\text{CH}}$ long-range correlations of strychnine (**5**) are observed in the spectrum; it will be noted that the discernability of the two-bond responses varies somewhat as a function of the nature of the proton multiplet in question. An investigation of the role of the proton multiplet character, and the size of the ${}^2J_{\text{CH}}$ and ${}^3J_{\text{HH}}$ correlations is on going and will be the subject of a further report.



2

The “visibility” of the modulation of the ${}^3J_{\text{HH}}$ coupling

reflected in the ${}^2J_{\text{CH}}$ correlations can be controlled by the user, in part, by the parameter J_{scale} utilized in the CIGAR-HMBC experiment (7). To illustrate the effect of varying the parameter J_{scale} , we have used 2-pentanone (**3**) as a model compound after the pioneering work of Reynolds and co-workers (9) in the development of the XCORFE pulse sequence. Figure 5 shows five panels containing the long-range correlations to the C3 resonance of 2-pentanone from the 1-methyl, 4-methylene, and 5-methyl resonances. The parameter J_{scale} was varied in the five experiments shown through 0, 6, 12, 18, and 24. It is readily apparent from these data that the ${}^3J_{\text{CH}}$ long-range correlation responses from the 1- and 5-methyl resonances are not impacted by the variation of the J_{scale} parameter. In contrast, the F_1 skew associated with the two-bond (${}^2J_{\text{CH}}$) correlation from the 4-methylene resonance to C3 introduced with the STAR operator becomes more pronounced as J_{scale} is increased.



3

Based on the limited range of experience presently available with the ${}^2J, {}^3J$ -HMBC experiment, the best optimization of the parameter J_{scale} is difficult to define with any degree of assurance. Empirically, however, we have generally seen the best results with the experiment when J_{scale} was optimized at about 15. Further studies will, however, be necessary to fully explore the consequences of varying J_{scale} with different types of molecules.

Finally, a question uniformly raised with the introduction of any new, and more complex long-range heteronuclear shift correlation experiment is the comparative sensitivity of the experiment relative to existing experiments such as HMBC/GHMBC (2, 3). In the past, we have partially addressed this question in a comparison of the results obtained using GHMBC, ACCORD-HMBC, and IMPEACH-MBC for the acquisition of long-range ${}^1\text{H}$ - ${}^{15}\text{N}$ heteronuclear shift correlation data at natural abundance (15). These data demonstrated that while the GHMBC experiment gave higher overall s/n (due to one very intense response), a comparison of individual responses showed the IMPEACH-MBC experiment to provide superior signal intensity for responses that were very weak in the GHMBC data while the response intensity for the high intensity response was only marginally lower (36:1 vs. 42:1) than the same response in the GHMBC spectrum. On this basis, we felt it most germane to draw comparisons of the relative performance from the various accordion-optimized long-range experiments now available vs. GHMBC on the basis of the H11 α -C12 and -C13 responses shown in the expanded panel of Fig. 4.

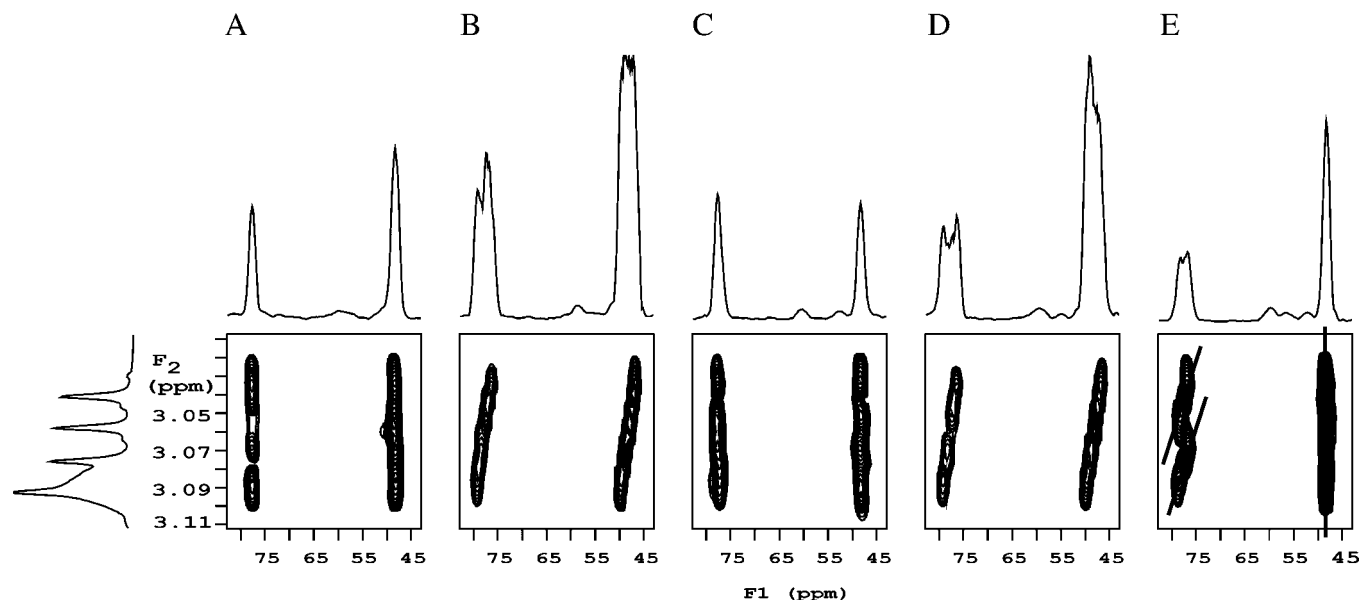


FIG. 6. Comparison of conventional GHMBC to accordion-optimized long-range heteronuclear shift correlation experiments. All data sets were accumulated as 2048×128 point files with 32 transients/ t_1 increment. No broadband heteronuclear decoupling was employed in the acquisition of any of the data, irrespective of whether the experiment allows this option. Data were linear predicted to 256 points in t_1 prior to Fourier transformation, and squared sinebell multiplication was employed in both time domains. Experiments performed included: (A) 8 Hz optimized GHMBC (91 min acquisition); (B) 6–10 Hz optimized ACCORD-HMBC (96 min acquisition); (C) 6–10 Hz optimized IMPEACH-MBC (99 min acquisition); (D) 6–10 Hz optimized CIGAR-HMBC, $J_{\text{scale}} = 16$ (97 min acquisition); (E) 6–10 Hz optimized ${}^2J, {}^3J$ -HMBC, $J_{\text{scale}} = 16$ (96 min acquisition). The identical regions of the aliphatic long-range correlation spectra show the correlations of the H-11 α to C-12 and C-13 via ${}^2J_{\text{CH}}$ and ${}^3J_{\text{CH}}$, respectively. The GHMBC (A) and IMPEACH-HMBC (C) data show slight modulation in F_1 due to homonuclear coupling modulation during the evolution time, t_1 . The ACCORD-HMBC spectrum (B) shows significant F_1 skew due to uncontrolled homonuclear coupling modulation occurring during the variable delay, which serves as a pseudo evolution period for these processes in addition to modulation during the evolution period (5). The CIGAR-HMBC data show user-controllable F_1 skew that can be adjusted as desired as a determinant of the authenticity of weak responses. The $J_{\text{scale}} = 16$ setting produces a considerable degree of skew but does not lead to any response overlap as is possible in the ACCORD-HMBC experiment. Finally, the ${}^2J, {}^3J$ -HMBC data (E) show the characteristic “staggered F_1 skew” of the ${}^2J_{\text{CH}}$ correlation of H11 α -C12 and no modulation of the ${}^3J_{\text{CH}}$ H11 α -C13 correlation response (other than that occurring due to the incrementation of the evolution time, t_1). Adjustment of the value of the parameter J_{scale} in this experiment affects only the characteristics of the ${}^2J_{\text{CH}}$ correlation responses as shown in Fig. 5. The projections through F_1 of the individual panels shown provide a signal-to-noise (s/n) comparison of the data in the five experiments performed. All of the projections were identically scaled. Previous work (15) has shown that more meaningful performance comparisons between “static” (single optimization, e.g. as with the GHMBC experiment) and accordion-optimized data are perhaps best obtained by comparing individual responses on an experiment-by-experiment basis as shown here. The data shown suggest that the newly reported ${}^2J, {}^3J$ -HMBC experiment affords performance that is comparable to that provided by the GHMBC experiment. A wider variety of molecules will, however, have to be examined comparatively using these experiments before a more definitive statement on the relative sensitivity of these experiments can be made with any degree of authority.

Comparative data are shown in Fig. 6 for the H11 α -C12 and H11 α -C13 (shown as projections through F_1) correlations from a series of identically parameterized long-range heteronuclear shift correlation spectra (insofar as is possible) of strychnine (**2**). Data are shown for an 8-Hz optimized GHMBC experiment, and the following 6–10 Hz accordion-optimized experiments: ACCORD-HMBC, IMPEACH-MBC, CIGAR-HMBC ($J_{\text{scale}} = 16$), and ${}^2J, {}^3J$ -HMBC ($J_{\text{scale}} = 16$). Digitization in both frequency domains was identical in all experiments; data acquisition times were comparable. Broadband heteronuclear decoupling was not applied in any of the accordion-optimized experiments, although this is an option for all but the ${}^2J, {}^3J$ -HMBC experiment in its present form.

As will be noted from the identically scaled projections plotted above each of the panels in Fig. 6, response intensity in the ${}^2J, {}^3J$ -HMBC data compares favorably with that from the

GHMBC experiment. The response intensity for ${}^2J, {}^3J$ -HMBC is somewhat lower than for the ACCORD-HMBC and CIGAR-HMBC experiments and better than for the IMPEACH-MBC experiment.

CONCLUSIONS

A new accordion-optimized long-range heteronuclear shift correlation experiment, ${}^2J, {}^3J$ -HMBC, capable of differentiating two-bond from three-bond couplings to protonated carbons has been reported. This is the first inverse-detected experiment to afford this capability since the heteronucleus-detected XCORFE pulse sequence developed by Reynolds and co-workers in 1985 (9). However, unlike the XCORFE experiment, the new ${}^2J, {}^3J$ -HMBC experiment offers two advantageous features. First, the experiment is accordion-optimized,

making it possible to sample a broad range of potential long-range couplings in a single experiment (4–7). Second, the use of the parameter J_{scale} makes it possible to augment the modulation in F_1 used to differentiate ${}^2J_{\text{CH}}$ from ${}^3J_{\text{CH}}$ responses. We feel that these features will make the ${}^2J, {}^3J$ -HMBC experiment more versatile and more widely applicable to the characterization of challenging, unknown chemical structures than any of the predecessor accordion-optimized experiments. Regrettably, the ${}^2J, {}^3J$ -HMBC experiment does not allow the differentiation of ${}^2J_{\text{CH}}$ from ${}^3J_{\text{CH}}$ responses to quaternary carbons since it relies on the operation of the BIRD pulse on the proton directly bound to the carbon of interest. In such cases, however, the use of long-range correlation responses from the ${}^2J, {}^3J$ -HMBC, or any other long-range heteronuclear correlation method, in conjunction with proton–proton homonuclear connectivity information should allow the differentiation of ${}^2J_{\text{CH}}$ from ${}^3J_{\text{CH}}$ correlations to quaternary carbons. In cases where sufficient material is available, investigators also have recourse to methods such as 1,1-INADEQUATE (16, 17). Finally, since the sensitivity of the experiment is comparable to that of the conventional HMBC/GHMBC experiments, it is hoped that ${}^2J, {}^3J$ -HMBC will gain acceptance among NMR spectroscopists engaged in structure elucidation.

REFERENCES

1. G. E. Martin and A. S. Zektzer, Long-range two-dimensional heteronuclear chemical shift correlation, *Magn. Reson. Chem.* **26**, 631–652 (1988).
2. A. Bax and M. F. Summers, ${}^1\text{H}$ and ${}^{13}\text{C}$ Assignments from sensitivity-enhanced detection of heteronuclear multiple bond connectivity by 2D multiple quantum NMR, *J. Am. Chem. Soc.* **108**, 2093–2094 (1986).
3. R. E. Hurd and B. K. John, Gradient-enhanced proton-detected heteronuclear multiple quantum spectroscopy, *J. Magn. Reson.* **91**, 648–653 (1991).
4. R. Wagner and S. Berger, ACCORD-HMBC: A superior technique for structural elucidation, *Magn. Reson. Chem.* **36**, S44–S48 (1998).
5. G. E. Martin, C. E. Hadden, R. C. Crouch, and V. V. Krishnamurthy, ACCORD-HMBC: Advantages and disadvantages of static vs. accordion optimization, *Magn. Reson. Chem.* **37**, 517–528 (1999).
6. C. E. Hadden, G. E. Martin, and V. V. Krishnamurthy, Improved performance accordion heteronuclear multiple-bond correlation spectroscopy—IMPEACH-MBC, *J. Magn. Reson.* **140**, 274–280 (1999).
7. C. E. Hadden, G. E. Martin, and V. V. Krishnamurthy, Constant time inverse-detection gradient accordion rescaled heteronuclear multiple bond correlation spectroscopy—CIGAR-HMBC, *Magn. Reson. Chem.* **38**, 143–147 (2000).
8. K. Furihata and H. Seto, Constant time HMBC (CT-HMBC), a new HMBC technique useful for improving separation of cross peaks, *Tetrahedron Lett.* **39**, 7337–7340 (1998).
9. W. F. Reynolds, D. W. Hughes, M. Perpick-Dumont, and R. G. Enriquez, A pulse sequence for establishing carbon-carbon connectivities *via* indirect ${}^1\text{H}$ – ${}^{13}\text{C}$ polarization transfer modulated by vicinal ${}^1\text{H}$ – ${}^1\text{H}$ coupling, *J. Magn. Reson.* **63**, 413–417 (1985).
10. V. V. Krishnamurthy, Phosphorus J-scaled band-selective homonuclear-decoupled TOCSY for $\text{H}3'$ - ${}^{31}\text{P}$ coupling constant measurement in DNA oligomers, *J. Magn. Reson. B* **113**, 46–52 (1996).
11. V. V. Krishnamurthy, Excitation-sculptured indirect-detection experiment (EXSIDE) for long-range CH coupling-constant measurement, *J. Magn. Reson. A* **121**, 33–41 (1996).
12. K. Furihata and H. Seto, J-Resolved HMBC, a new NMR technique for measuring heteronuclear long-range coupling constants, *Tetrahedron. Lett.* **40**, 6271–6275 (1999).
13. P. Permi, I. Kilpeläinen, and S. Heikkinen, An improved J-multiplied method for the measurement of ${}^3J(\text{H}^{\text{N}}, \text{H}^{\text{C}})$ from the two-dimensional ${}^{15}\text{N}$ – ${}^1\text{H}$ correlation spectrum, *Magn. Reson. Chem.* **37**, 821–826 (1999).
14. R. T. Williamson, B. L. Márquez, W. H. Gerwick, and K. E. Kövér, One and two dimensional gradient-selected HSQMBC NMR experiments for the efficient analysis of long-range heteronuclear coupling constants, *Magn. Reson. Chem.* **38**, 265–273 (2000).
15. G. E. Martin and C. E. Hadden, Applications of accordion excitation in ${}^1\text{H}$ – ${}^{15}\text{N}$ long-range heteronuclear shift correlation experiments at natural abundance, *Magn. Reson. Chem.* **38**, 251–256 (2000).
16. B. Reif, M. Köch, R. Kerssebaum, J. Schlecucher, and C. Griesinger, Determination of 1J , 2J , and 3J carbon–carbon coupling constants at natural abundance, *J. Magn. Reson. B* **112**, 295–301 (1996).
17. M. Köch, B. Reif, W. Fenical, and C. Griesinger, Differentiation of HMBC two- and three-bond correlations: A method to simplify structure determination in natural products, *Tetrahedron Lett.* **37**, 363–366 (1996).